JOURNAL OF OPTOELECTRONICS AND ADVANCED MATERIALS, Vol. 12, No. 6, June 2010, p. 1421 - 1426

Optical properties of sol-gel prepared nano ZnO. The effects of modifier and hydrolysis agent

A. ESMAIELZADEH KANDJANI[a*], M. FARZALIPOUR TABRIZ[a], N.A. AREFIAN[a], M.R. VAEZI[a], S. AHMADI KANDJANI[b]
[a]*Materials and Energy Research Center (MERC), Karaj, Iran*
[b]*Research Institute for Applied Physics and Astronomy, University of Tabriz, Tabriz, Iran*

Zinc oxide nanoparticles were synthesized via Sol-Gel method from zinc acetate as precursor and thriethanolamin (TEA) as modifier. The crystal structures and morphology of the nanoparticles were investigated using X-ray Diffractometer (XRD) and Transition Electron Microscope (TEM) respectively. The optical band gaps were estimated from UV-Vis spectrophotometery analysis. The results show strong dependence of the optical band gap on the synthesis conditions. The effects of $Zn(Ac)_2$/TEA and water/ethanol ratios on properties of obtained zinc oxide nanoparticles were investigated. The band gap changes slightly with the modifier amount, while the internal strain and, thus, Urbach energy change drastically. An increase in water amount in sol-gel process decrease the crystallite size, while structural microstrain and optical properties of the samples i.e. band gap and Urbach energy, are highly dependent on ratio water/ethanol.

(Received March 2, 2010; accepted June 17, 2010)

Keywords: ZnO; Sol-Gel; Band gap; Interior micro-strain; Urbach energy

1. Introduction

Optoelectronics and its related technologies have been boosted by emerging nano-materials. Due to their properties arisen from quantum confinement effects, these materials have become main attraction in many research areas. Among the nano semiconductors materials, ZnO is found to be suitable material for optoelectronic applications, including: blue light emitting diodes (LED) [1], photocatalyst [2], transistor [3], etc. Zinc oxide has a wide band gap of ~3.3eV (at bulk state), low resistivity and high transparency in visible light wavelengths and also high light trapping characteristics [4], which ensures its efficient ultraviolet (UV) emission up to room temperature [5]. Hexagonal wurtzite (a=3.25Å and c=5.12Å) is the main stable crystalline structure of ZnO at room temperature [6].

The properties of semiconductors mainly depend on their band structures. In electrical and optical applications, a certain band structure is needed and thus investigation on the effects of involving parameters on semiconductors band structure has become vital in these applications. The band structure of semiconductors is highly dependent on their crystalline structure. Thus, the influence of the synthesis method's parameters on the final crystalline structure can influence the band structure of obtained material. It is known that the introduction of a high concentration of defects and impurities in perfect semiconducting crystals causes a perturbation of the band structure with the result that the parabolic distribution of the states will be distributed and prolonged by a tail extending into the energy gap [7]. The different synthesis conditions can result in different amounts of localized strains. Non-homogeneous distribution of defects results in stronger or weaker local interactions which will also influence the band edges. Therefore, one of the main challenges among researchers is to investigate the effects of synthesis variables on the final properties of semiconductors.

Many chemical methods have been used for obtaining ZnO nanoparticles, including: hydrothermal [8], reverse micelles [9], sol-gel [10], direct chemical synthesis [11], sonochemical [12], etc. Among these synthesis routes, sol-gel is one of the well known methods due to its easy procedure, high film thickness controllability, low-cost and coating ability of large complex shaped substrates. Various parameters, including temperature, medium pH, aging period, amount and type of modifier and hydrolysis agent, can change the morphology and crystal structure of final products as well as their band structures [13].

In our previous work [14], the effects of aging period and synthesis temperature on final properties of ZnO nano particles as well as related sol-gel mechanisms, were reported. In this paper, the effects of two other important variables; i.e. modifier and hydrolysis agent has been reported.

2. Experimental

2.1. Materials

Analytical grade $Zn(Ac)_2.2H_2O$, triethanolamine (TEA) and ethanol were purchased from Merck and used without further purification.

2.2 Synthesis method

First, 0.1 molar $Zn(Ac)_2$ aqueous solution was prepared and desired amount of TEA was dissolved in absolute ethanol separately. Both vessels were kept at 60°C in a heating-cooling bath and then the solutions were mixed to prepare 50 ml solutions with specifications shown in Table 1. After obtaining white solution, the prepared samples were gathered and dried at 60°C for 24hr. Finally all samples were annealed at 400°C for 1hr.

Table 1. Synthesis condition of samples.

Sample	Volume of Water/Ethanol [ml]	Weight Ratio of $Zn(Ac)_2$/TEA
Z-1	25/25	0.5
Z-2	25/25	1
Z-3	25/25	2
Z-4	13/37	1
Z-5	37/13	1

2.3. Analyses

The crystalline structures of materials were studied using a Siemens D-5000 X-ray diffractometer (XRD) with Cu-K_α radiation (λ= 0.154178 nm). Scanning Electron Microscopy (Philips XL30) and Transmission Electron Microscopy (Philips CM200) images were used for studying morphology of the prepared samples. Optical properties were studied by double-beam Shimadzu UV-2450 Scan UV-Visible spectrophotometer.

2.4. Used equations

Average crystallites sizes of particles were estimated from the full width at half maximum (FWHM) of the highest X-ray diffraction peak angels using the Debye–Scherrer formula [15]:

$$D = \frac{k\lambda}{\beta \cos\theta} \tag{1}$$

where D is the mean crystallite size; k is a grain shape dependent constant (here assumed to be 0.89 for spherical particles); λ is the wavelength of the incident beam; θ is the Bragg peak; and β is the full width of half maximum.
The internal micro strains of samples has been estimated using Williamson-Hall relation [16]:

$$\beta \cdot Cos\theta = \frac{k\lambda}{D} + \varepsilon \cdot Sin\theta \tag{2}$$

where β is full width at half maximum (FWHM) of (100), (002), (101), (102) and (103) reflections of ZnO, k is the Scherrer constant, D is average crystallite size, λ is the wavelength of irradiated X-Ray, θ is the Bragg angle and ε is the internal microstrain.

Absorption coefficients of colloidal ZnO suspension (α, cm^{-1}) have been calculated using the following equation [17]:

$$\alpha = 2303\left(\frac{D.\rho}{C.l}\right) \tag{3}$$

where, D is the optical density of solution, ρ is the density of bulk ZnO crystals ($5.606\, g/Cm^3$) [6], C is the ZnO concentration (g/Cm^3) and l is the optical path (cm).

Absorption coefficient of semiconductors, $\alpha(\lambda)$, which is mentioned in Eq. (3), is given by the following expression [17]:

$$\alpha = A\frac{\left(h\nu - E_g\right)^n}{h\nu} \tag{4}$$

where A is coefficient of given electronic transition probability and n is equal to 0.5 and 2 for allowed direct and indirect transitions and 1.5 and 3 in case of forbidden direct and indirect transitions, respectively.

Near band edge, the absorption coefficient, α, varies exponentially with photon energy. We can assume that the spectral dependence of the absorption edge is in accordance to Urbach formula [18]:

$$\alpha(h\nu) = \alpha_0 \cdot \exp\left[\frac{(h\nu)}{E_0}\right] \tag{5}$$

where α_0 is the Urbach absorption at the edge and E_0 is the Urbach energy width which weakly depends on temperature and is believed to be a function of the structural disorder. The exponential dependence of the absorption on $h\nu$ in the Urbach region ($h\nu < E_g$) is due to the perturbation of the parabolic density of the states at the band edge increasing structural disorder results in an increase in E_0 [19].

The procedure for obtainning n, E_g and E_0 are explained thoroughly in our previous paper [14].

3. Results and discussion

3.1. The effects of modifier

XRD patterns of samples Z-1, Z-2 and Z-3 are shown in Fig. 1. All peaks are attributed to wurtzite ZnO (JCPDF 36-1451) and no peaks of other crystalline phases were detected. As it can be seen in this figure, diffraction peaks from (002) planes have the highest intensity and the intensity orders of peaks are similar in these samples.

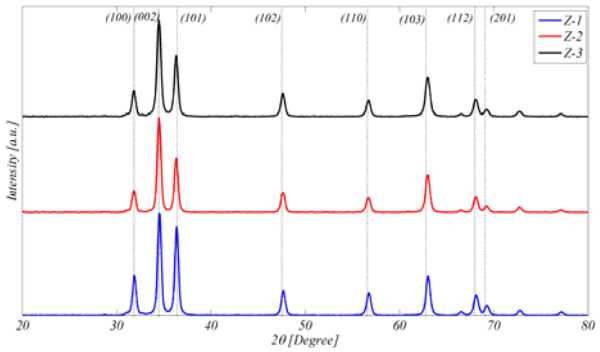

Fig. 1. XRD pattern of samples Z-1, 2 and 3.

TEM images of these samples showed a semi spherical morphology for all of them with no noticeable change in morphology by variation in modifier amounts. Also selected area electron diffraction (SAED) analysis showed crystalline ZnO structure. The TEM image of sample Z-2 and its SAED pattern are shown in Fig. 2.

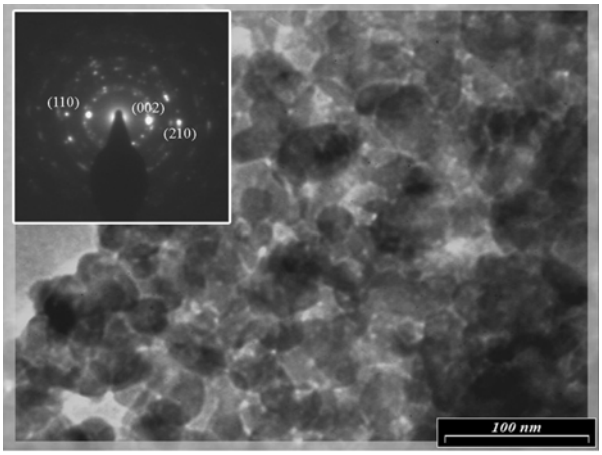

Fig. 2. TEM image and SAED pattern of sample Z-2.

From Eq. (2) the average crystallites size of the samples are estimated as shown in Fig. 3. Decrease in the amount of TEA, results in increase of crystallites size of the zinc oxide particles. The main role of TEA as a modifier is to prolong the hydrolysis process which consequently leads to formation of smaller sol particles and better dissolution of precursors in the sol gel media [20,21]. These phenomena can be extremely intensified by increasing the amount of TEA. When sufficient amounts of TEA is provided for zinc complexes, the process can be followed by reactions including hydrolysis, sol formation and polymerization or condensation of sols which the rate of the reactions can be controlled by varying the amounts of modifier. The joining of zinc initial positive charged complex, which were made by contribution of zinc ions and TEA atoms, increases the molecular complexity. By increase in molecular complexity the rate of hydrolysis decreases [13] so smaller particles are produced at lower ratios of $Zn(Ac)_2$/TEA.

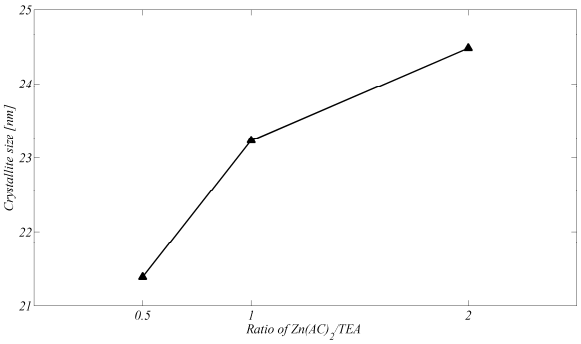

Fig. 3. The average crystallites size of zinc oxide particles vs. amounts of modifier.

The UV absorbance spectra of obtained samples are illustrated in Fig. 4. The absorbance spectra of obtained ZnO samples show an intense change in 360 to 400nm range. A large shoulder can be seen in the absorbance spectra of these samples. This excitonic peak is related to the quantum confinement effect due to nanoscopic size of the crystallites [22].

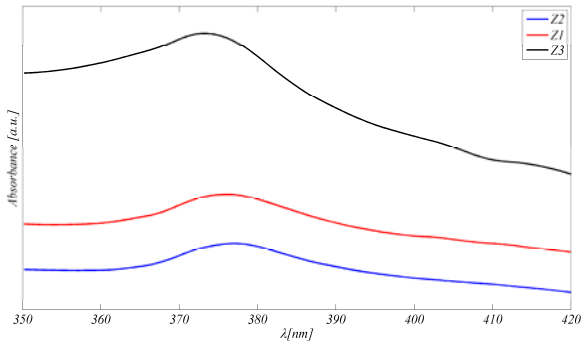

Fig. 4. UV-Vis absorbance spectra for samples Z-1, 2 and 3.

Band gap values of samples are estimated from absorbance spectra by using Eq. (4). The variations of band gap value by $(Zn(Ac)_2/TEA)$ are shown in Fig. 5. In comparison with band gap value of ideal bulk ZnO i.e. 3.3eV, all samples have less band gap values.

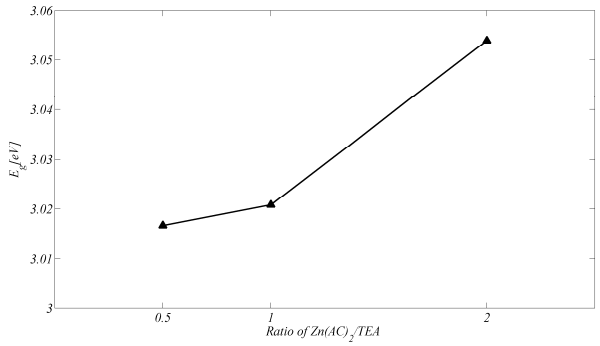

Fig. 5. Dependence of band gap value to $Zn(Ac)_2/TEA$.

This might be due to the internal micro-strain arising from chemical synthesis of ZnO and short duration of annealing. These micro-strains highly influence the optical band gap of material [23]. The micro-strain of the samples estimated from Eq. (3), increase by increasing ratio of $Zn(Ac)_2/TEA$ as shown in Fig. 6. The smaller particles dissolve and precipitate onto larger particles. This mechanism is called Ostwald ripening whereby particles grow in size and decrease in number as highly soluble small particles dissolve and reprecipitate on larger, less soluble ones. Growth stops when the difference in solubility between the smallest and largest particles becomes only a few ppm. This process tends to increase the crystallite size of samples. The strained regions in materials tend to solute faster than stress-free areas so solution-precipitation process results in lowering the total micro-strains in prepared samples [24].

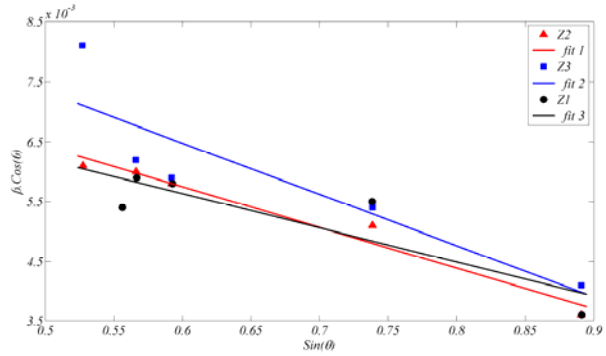

Fig. 6. Internal microstrain vs. $(Zn(Ac)_2/TEA)$.

By decreasing the precipitation rate of zinc oxide nanoparticles, the structures of obtained particles are much more likely to be perfect. Also due to Ostwald ripening which is based on resolving and re-nucleation of particles which itself depends on temperature and aging period, the samples which has low ratio of $Zn(Ac)_2/TEA$ and thus lowers synthesis rates show less disordering in their structures. This phenomenon can affect the E_0 of the samples as shown in Fig. 7. E_0 values decrease as the strains in the materials decrease which can subsequently influence the optical properties of the material.

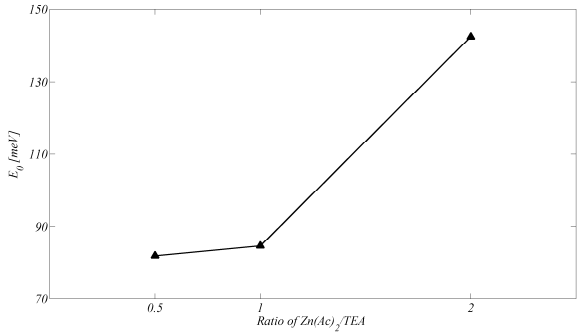

Fig. 7. Dependence of Urbach energy to $Zn(Ac)_2/TEA$.

According to the estimated values for micro-strains and crystallites sizes of the samples, band gap values of samples increase by increasing $Zn(Ac)_2/TEA$ as shown in Fig. 5.

3.2. The effects of hydrolysis agent

XRD patterns of samples Z-2, Z-4 and Z-5 are shown in Fig. 8. All peaks are attributed to wurtzite ZnO (JCPDF 36-1451) and no peaks of other crystalline phases were detected.

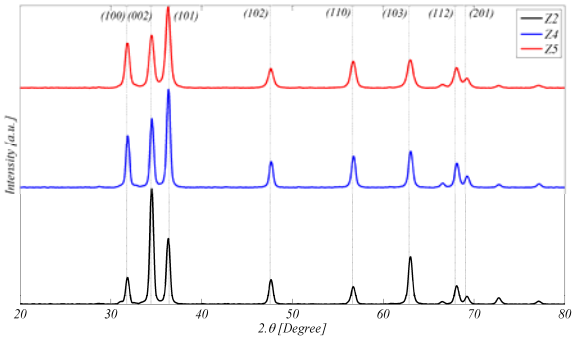

Fig. 8. XRD pattern of samples Z-2, 4 and 5.

The average crystallite size variation with increasing the water amounts of water is shown in Fig. 9. An increase in water amount results in a decrease in crystallite size, as could be seen in this figure.

For coordinatively saturated metal ions in sol gel, i.e. high molar ratios of water:metal, hydrolysis and condensation both occur by nucleophilic mechanisms (S_N), including nucleophilic addition (A_N), proton transfers from the attacking molecule to an alkoxide within the transition state [13].

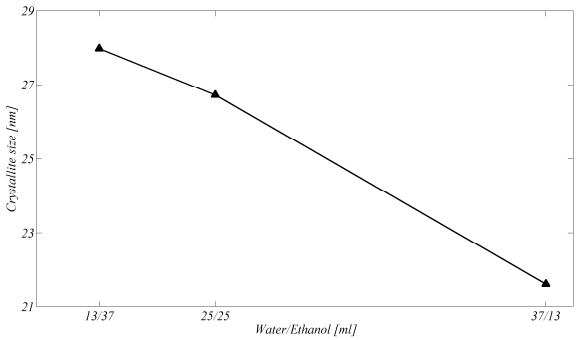

Fig. 9. Variations of average crystallite size of zinc oxide particles vs. water/ethanol ratio.

Thus, the mechanisms of synthesis can be carried out by hydrolysis of sol gel derived zinc alkoxides, alkoxolation, oxolation or in high amounts of water olation reaction process. The olation process is highly depends on amounts of water/alcohol ratio [25]:

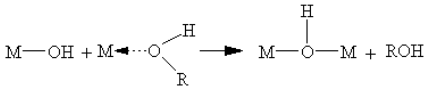

(6)

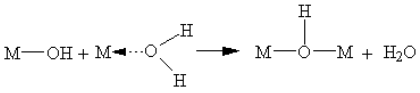

(7)

Wherein, M is related to metal ion. Thus the amount of hydrolysis agent (H_2O) is highly changes the reactions dealing with ZnO production. This could be arisen from different attacking solvents as could be seen in Eq. (6) and (7). When proportion of water increases in solution the rate of hydrolysis reactions increases. This phenomenon leads to increase in nucleation rates and thus the amount of stable nuclei increases the in synthesis solution [25]. Therefore, smaller particles are produced.

The UV absorbance spectra of samples Z-2, Z-4 and Z-5 are illustrated in Fig. 10. As previous samples, the absorbance spectra of obtained ZnO samples have an intense change in the 360 to 400 nm range.

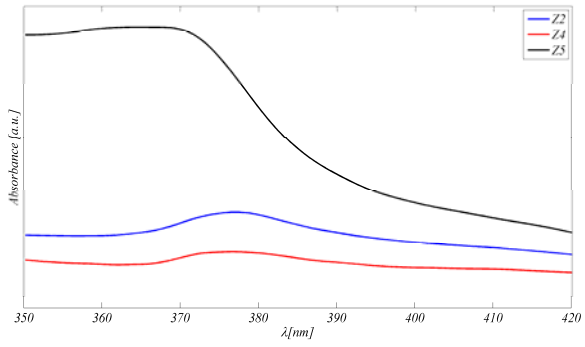

Fig. 10. UV-Vis absorbance spectra for samples Z-2, 4 and 5.

The band gaps of synthesized samples were calculated using Eqs. (3) and (4) based on absorption spectra of Fig. 10. The results are illustrated in Fig. 11. As could be seen in this figure by increase in ratio of water/ethanol the band gap decrease slightly but in higher amounts of water a considerable increase in band gap was detected.

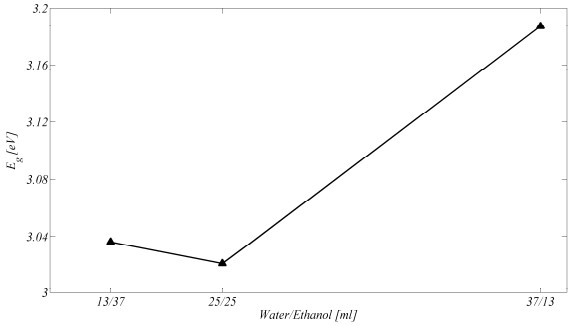

Fig. 11. Dependence of band gap to water/ethanol ratio.

The calculated changes of interior strains by changing amounts of water in sol gel solution are shown in Fig. 12. As could be seen from this figure, when ethanol and water have same portion in the solution the interior micro strain has maximum values, while when water constitutes major portion of synthesis solution, minimum interior micro-strain is gained.

When ethanol is higher than water in the synthesis, Olation mechanisms of synthesis tends to Eq. (6). By increase of the water amount the reaction via Eq. (7). When the ratio of water to ethanol increases, the solubility increases which results in increasing Ostwald ripening phenomenon and reduction of internal strains. When water and ethanol have the same proportion in solution, the reaction could be happen via either Eq. (6) or Eq. (7), which exerts excess strain by the incoherent production of ZnO particles due to contribution of both mechanisms.

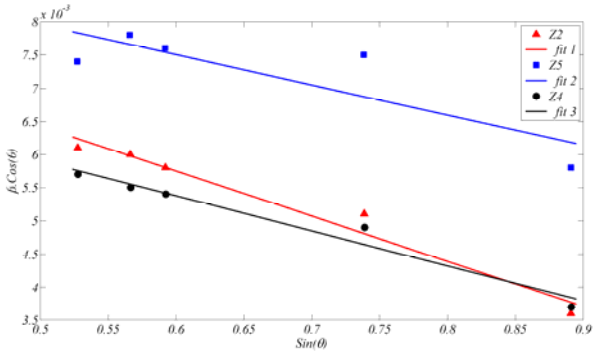

Fig. 12. Internal microstrain vs. water/ethanol ratio.

The internal micro-strain can influences the electrical state of the material. This phenomenon can be detected by Urbach energy variation. Fig. 13 illustrates the variation of Urbach energy by increasing the ratio of water/ethanol. As could be seen the results show a good consistency between internal micro-strains and Urbach energies of the samples. The obtained properties are shown in Table 2.

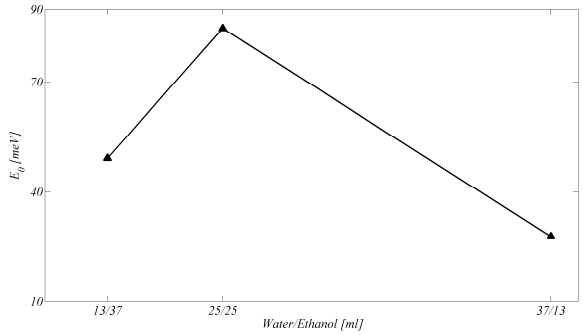

Fig. 7. Dependence of Urbach energy to water/ethanol ratio.

Table 2 the obtained properties of the synthesized samples.

Sample	Average crystallite size (nm) [±0.05]	Band gap (eV) [±0.05]	Urbach energy (meV) [±0.5]
Z-1	25.17	3.01	78.1
Z-2	26.72	3.02	84.7
Z-3	26.91	3.08	142.5
Z-4	27.97	3.04	49.2
Z-5	21.63	3.19	27.7

4. Conclusions

In present work, ZnO nanoparticles were synthesized via Sol-Gel method. The effects of modifier and hydrolysis agent on the optical band gap were investigated. The crystallite size and the band gap of obtained nanoparticles varied from 21.63nm to 27.91nm and 3.02eV to 3.27eV, respectively. Also the Urbach widths of ZnO nanoparticles were varied from 27.7meV to 142.5meV. The results show that the water/ethanol ratio has the highest influence on the crystallite size and internal microstrain which is led to expand in Urbach energy width. Thus, the microstrain and quantum size effects are in competition with each other and these two phenomena must be considered together for investigating on optical band gap of semiconductors.

References

[1] X. M. Zhang, M. Y. Lu, Y. Zhang, L. J. Chen, Z. L. Wang, Adv. Mater. **21**, 2767 (2009).
[2] B. Pal, M. Sharon, Mater. Chem. Phys. **76**, 82 (2002).
[3] H. Yuan, H. Shimotani, A. Tsukazaki, A. Ohtomo, M. Kawasaki, Y. Iwasa, Adv. Funct. Mater. **19**, 1046 (2009).
[4] L. Xu, Y. Su, Y.Q. Chen, H.H. Xiao, L.A. Zhu, Q. T. Zhou, S. Li, J. Phys. Chem. B **110**, 6637 (2006).
[5] R. Deng, X. T. Zhang, J. Lumin. **128**, 1442 (2008).
[6] D. P. Norton, M. Ivill, Y. Li, Y.W. Kwon, J. M. Erie, H. S. Kim, K. Ip, S. J. Pearton, Y. W. Heo, S. Kim, B. S. Kang, F. Ren, A.F. Hebard, J. Kelly, Thin Solid Films **496**, 160 (2006).
[7] D. A. Drabold, S. Estericher, Theory of defects in semiconductors, Springer, Germany, (2007).
[8] Y. Hu, H.J. Chen, J. Nanopart. Res. **10**, 1369 (2008).
[9] T. Hirai, Y. Asada, J. Colloid. Interf. Sci. **28**, 184 (2005).
[10] M. Ristic, S. Music, M. Ivanda, S. Popovic, J. Alloy. Compd. **397**, L1 (2005).
[11] C. Wu, X. Qiao, J. Chen, H. Wang, F. Tan, S. Li, Mater. Lett. **6**, 1828 (2006).
[12] A. Esmaielzadeh Kandjani, M. Farzalipour Tabriz, B. Pourabbas, Mater. Res. Bull. **43**, 645 (2008).
[13] C. J. Binker, G. W. Scherer, Sol-Gel Science: The physics and Chemistry of Sol-Gel Processing, Academic Press Inc., UK, (1990).
[14] A. Esmaielzadeh Kandjani, A. Shokuhfar, M. Farzalipour Tabriz, N.A. Arefian, M.R. Vaezi, J. Optoelectron. Adv. Mater. **11**, 289 (2009).
[15] B. D. Cullity, Elements of X-ray Diffraction, 2nd ed., Addison-Wesley Company, USA, (1978).
[16] C. Suryanaryana, M. G. Norton, X-ray diffraction: A practical approach, Plenum Press, USA, (1998).
[17] S. V. Gaponenko, Optical Properties of Semiconductor Nanocrystals. Cambridge: University Press, (1996).
[18] F. Urbach, Phys. Rev. **92**, 1324 (1953).
[19] N. B. Chen, H. Z. Wu, D. J. Qiu, T. N. Xu, J. Chen, W. Z. Shen, J. Phys. Condens. Matter. **16**, 2973 (2004).
[20] L. Znaidi, G.J.A.A. Soler Illia, S. Benyahia, C. Sanchez, A.V. Kanaev, Thin Solid Films **428**, 257 (2003).
[21] Z. Liu, Z. Jin, W. Li, J. Qiu, Mater. Lett. **59**, 3620 (2005).
[22] E. A. Meulenkamp, J. Phys. Chem. B **102**, 5566 (1998).
[23] V. Srikanth, D.R. Clarke, J. Appl. Phys. **81**, 6357 (1997).
[24] O. Sohnel, J. W. Mullin, J. Colloid. Interf. Sci. **123**, 43 (1988).
[25] D. L. Marchisio, F. Omegna, A. A. Barresi, P. Bowen, Ind. Eng. Chem. Res. **47**, 7202 (2008).

*Corresponding author: MSTGAhmad@Gmail.com